2024 IEEE International Conference on Robotics and Automation (ICRA 2024)
May 13-17, 2024. Yokohama, Japan

OSCaR: An Origami-Inspired Shape-Changing Robot for Ground Coverage Tasks

Zirui Fan[1], and Hongying Zhang[2*], *IEEE Membership*

***Abstract*— This paper introduces a novel origami-inspired shape-changing robot OSCaR. The objective is to enhance the adaptability of vehicles engaged in ground coverage tasks, such as floor cleaning. The robot exhibits two distinct configurations: it can fold itself for agile navigation through tight spaces, and unfold to cover larger areas efficiently. The folding pattern has a deploy-to-stow ratio of 3 in the width dimension, and a kinematic model is established to simulate the deployment process for the pattern. The hinge design employs rolling contact elements to mitigate collision among the panels, particularly in regions with multiple colinear crease lines. Furthermore, the design exhibits one degree of freedom and features pivots, making it easy to actuate with motors. The system design of the prototype is also presented, including its structure, an embedded hardware system, and upper computer software. The results show that the robot has great adaptability in complex environments.**

I. Introduction

Ground mobile robots are specifically engineered to traverse and operate in land-based settings, encompassing a wide spectrum of terrains, from open and wide spaces to tight and narrow paths. In terms of the type of work performed, ground mobile robots can be categorized into two primary classes: robots designed for point-to-point traversal and those intended for expansive area coverage. The former category encompasses instances such as delivery robots, which are tasked with transporting packages from suppliers to customers. The latter group includes floor cleaning robots, designed to efficiently cover designated areas for cleaning purposes. For the latter category, the coverage efficiency is proportional to the robot's movement speed and the reciprocal of its width. Elevating either of these parameters can result in improved efficiency. Given that locomotion speed is contingent upon the locomotion system itself, the best way to improve coverage efficiency is by increasing the robot's width. However, as the robot's width increases, its maneuverability gets reduced, particularly in confined spaces. To address this problem, the integration of shape-changing mechanisms emerges as a viable resolution. Incorporating shape-changing capabilities allows robots to reconfigure themselves in constrained spaces, thereby enhancing their agility, while also being able to expand to optimize coverage in more open areas.

One approach for designing such adaptable shape-changing structures is drawing inspiration from the art of origami. Origami structures are deployable, scalable [1], and especially, able to fit large structures into small packages [2], making them suitable for applications in various fields, such as aerospace [3], [4], architecture [5], manufacturing [6], medicine [7], [8], and robotics [9]–[14]. Notable examples include the deployable solar array by Zirbel *et al.* [4], which is highly compact and has a deploy-to-stow ratio of 9.2, and the pop-up rover PUFFER [11] by NASA, which can nearly halve its height through folding. These attributes render origami structures ideally suited for the development of shape-changing mobile robots that seek to adeptly navigate both spacious and confined environments.

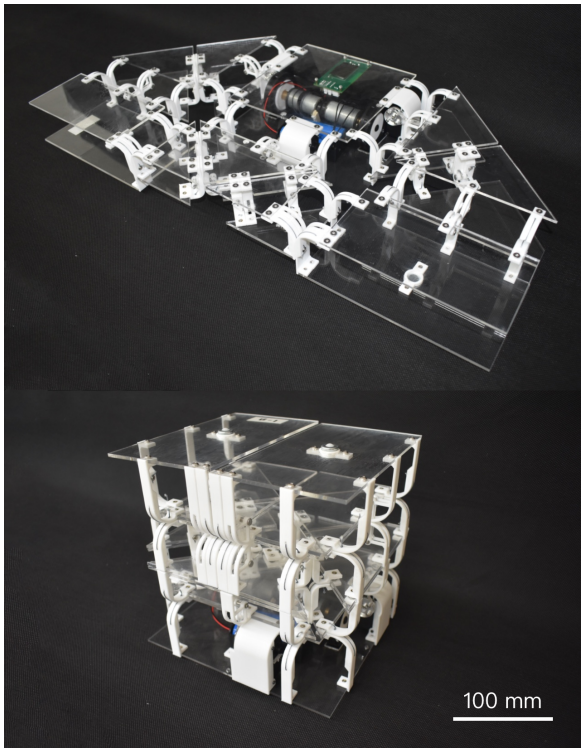

Fig. 1. Functional prototype of OSCaR in the deployed and folded configuration.

Numerous implementations of shape-changing structures have been introduced within the domain of wheeled mobile robots. These robots possess the capability to dynamically alter their physical configuration, allowing them to adapt to diverse environments and tasks, such as tunnels [15], complex working environment [16] and uneven terrain [9], [17]. The shape-changing structures offer advantages in area coverage [16], maneuverability [15], and obstacle clearance

[1]National University of Singapore (Suzhou) Research Institute, Suzhou, China.
[2]Department of Mechanical Engineering, National University of Singapore, Singapore.
*Corresponding author: Hongying Zhang, hy.zhang@nus.edu.sg

[9], [11], [17] compared to traditional wheeled platforms. Prior research has explored various mechanisms for shape transformation, including modular reconfiguration [18], foldable structures [9], [11], and deformable wheels [9], [17].

It is noteworthy that although existing designs of shape-changing mobile robots are able to enhance coverage or mobility, they all only dedicate focus to one of these aspects. For instance, hTetro [16] aimed at the maximization of coverage area. although it can get through narrow spaces by adopting an "I" configuration, its increased length hinders its agility of turning in those areas, leading to reduced maneuverability. In real-world environments, mobile robots must function adeptly within both confined and open spaces. Consequently, there exists a compelling need for the development of shape-changing robotic systems that effectively reconcile these dual operational demands.

In this paper, an origami-inspired shape-changing robot OSCaR (Fig. 1) is proposed. The main objective is to enhance the adaptability of ground vehicles that are designed for area coverage, by allowing them to fold themselves to better navigate through tight spaces and unfold to cover a larger area.

The contributions of this paper include:

- a compact folding structure that has a deploy-to-stow ratio of 3 in the width dimension;
- a kinematic model to simulate the shape-changing process of the proposed origami structure and provide guidance for actuation; and
- an easy-to-actuate collision-free hinge design for complex thick-panel folding.

The rest of this paper is organized as follows. Section II introduces the design rationale of the folding pattern and the hinge design. Section III presents the design of the prototype. Section IV shows the experiments on the prototype and discusses the robot's limitations. Finally, section V concludes the paper and discusses future work.

II. Design Rationale

A. Folding Pattern

The objective of this shape-changing robot is to enhance its adaptability in complex environments that have tight and narrow spaces. To achieve this goal, the folding pattern must exhibit a high deploy-to-stow ratio along the width dimension, as mentioned previously.

Additionally, the crease pattern design must ensure that the geometric center of the pattern remains within the perimeter of the part that is in constant contact with the ground throughout the folding process. This requirement ensures that the robot will not overturn during the folding process, as the center of mass of the robot is likely to be close to the geometric center.

The proposed pattern has a deploy-to-stow ratio of 3, as presented in Fig. 2 (a). The geometric center stays within the square region, which has constant contact with the ground. Therefore, the requirement is satisfied.

By adding thickness to the pattern, the folding pattern in Fig. 2 (a) results in the design shown in Fig. 2 (b). To accommodate the thickness, the mountain creases are shifted to the lower edges, while the valley creases are shifted to the upper edges of the panels when viewed in the deployed configuration.

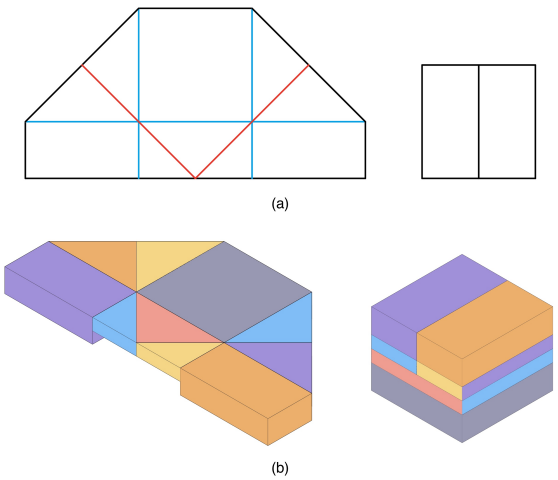

Fig. 2. Folding pattern design and thickness accommodation of OSCaR. (a) Basic folding pattern design in the deployed and folded state; Mountain folds are in red and valley folds are in blue. (b) Thick-panel model in the deployed and folded configuration.

B. Kinematic Model

The modeling of origami structures typically relies on the premise of rigidly foldable hypotheses [19], wherein deformation occurs while the facets remain undeformed. Therefore, creases can be modeled as joints and the facets can be represented as links, and the D-H (Denavit–Hartenberg) model can be utilized to describe the structures. Under these conditions, rigid body kinematics is then used to analyze the structures [20], [21]. Additionally, for thick-panel structures, a reduced degree of freedom is often observed due to overconstraint [22].

As shown in Fig. 3 (a), the thick-panel pattern in this project can be modeled as 2 plane-symmetric Bricard linkages coupled together. Since the 2 linkages are symmetric, their kinematics would be identical. Fig. 3 (b) shows the frame assignments and corresponding parameters of the $(i-1)$-th link. Each of the axes Z_i is directed along the ith crease, and each of the axes X_i is directed along the common normal from Z_{i-1} to Z_i, i.e. $X_1 = Z_6 \times Z_1$ and $X_i = Z_{i-1} \times Z_i$ for $i = 2, 3, .., 5$. α_i is the angle from Z_i to Z_{i+1} about X_i; a_i is the distance from Z_i to Z_{i+1} along X_i; d_i is the distance from X_{i-1} to X_i along Z_i, which is 0 for all cases since the frames are assigned to the vertices of each panel; θ_i is the angle from X_{i-1} to X_i about Z_i, which is the folding angle of each crease. The D-H model for one of the Bricard linkages is obtained by applying the D-H notations to all of the links, as shown in Fig. 3 (c). Frame 0 is set on the square panel of the structure. Since Z_6 intersects with Z_1 and Z_3 intersect with Z_4, X_1 is set to be $Z_6 \times Z_1$ and X_4 is set to be $Z_3 \times Z_4$. The D-H parameters are shown in TABLE I.

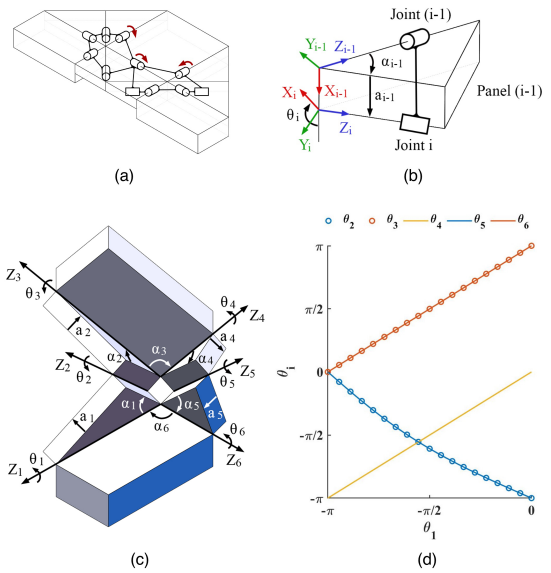

Fig. 3. Mathematical modeling of the folding pattern. (a) Equivalent linkage model of the folding pattern and the actuation scheme. (b) Frame assignments and corresponding parameters of the $(i-1)$-th link using D-H notations. (c) Frame assignments and corresponding parameters of a single linkage loop using D-H notations. (d) Joint angles of a single linkage loop during the folding process.

TABLE I
D-H PARAMETERS OF A SINGLE LINKAGE LOOP FROM THE PROPOSED FOLDING STRUCTURE

i	α_i	a_i	d_i	θ_i
1	$\pi/4$	h	0	θ_1
2	$-\pi/4$	h	0	θ_2
3	$\pi/2$	0	0	θ_3
4	$\pi/4$	h	0	θ_4
5	$-\pi/4$	h	0	θ_5
6	$\pi/2$	0	0	θ_6

As the links are connected end to end in a loop, the linkage satisfies the loop closure constraint

$$\boldsymbol{T}_2^1\boldsymbol{T}_3^2\boldsymbol{T}_4^3\boldsymbol{T}_5^4\boldsymbol{T}_6^5\boldsymbol{T}_1^6 = \mathbf{I} \tag{1}$$

where $\boldsymbol{T}_i^{i-1}$ is the homogeneous transformation matrix between link $(i-1)$ and link i, i.e.

$$\boldsymbol{T}_i^{i-1} = \begin{bmatrix} \cos\theta_i & -\sin\theta_i & 0 & \mathrm{a}_{i-1} \\ \sin\theta_i\cos\alpha_{i-1} & \cos\theta_i\cos\alpha_{i-1} & -\sin\alpha_{i-1} & -\sin\alpha_{i-1}\mathrm{d}_i \\ \sin\theta_i\sin\alpha_{i-1} & \cos\theta_i\sin\alpha_{i-1} & \cos\alpha_{i-1} & \cos\alpha_{i-1}\mathrm{d}_i \\ 0 & 0 & 0 & 1 \end{bmatrix} \tag{2}$$

By solving Equation 1, the kinematic motion can be derived.

Equation 1 can be rearranged into

$$\boldsymbol{T}_2^1\boldsymbol{T}_3^2\boldsymbol{T}_4^3\boldsymbol{T}_5^4\boldsymbol{T}_6^5\boldsymbol{T}_1^6 - \mathbf{I} = \mathbf{O} \tag{3}$$

Since the plane-symmetric Bricard linkage has one degree of freedom, Equation 3 would have only one root. In this paper, Equation 3 was numerically solved using the *fsolve* function in *MATLAB*, and the resultant joint angles during the folding process are shown in Fig. 3 (d). The results reveal that there exist linear relationships among the movements of joints 1, 3, 4, and 6, and their angular velocities are identical, whereas the movements of joints 2 and 5 are non-linear to the others but identical to each other.

Note that panels 5 and 6 in Fig. 3 are shared with the corresponding panels on the other half of the robot, thereby establishing an interdependence in the movements of the two linkages. Given that one linkage has one degree of freedom, the coupled linkages would also have one degree of freedom. However, in order to avoid singularities in the unfolded configuration, at least 3 actuators are required. To optimize the weight distribution, the actuators are designed to be placed inside the square panel, and the three actuated joints are highlighted with red arrows in Fig. 3 (a). According to the kinematic analysis, these three joints rotate at the same speed during the folding process.

C. Hinge

In Fig. 2, the folding pattern folds along ideal crease lines without considering the structural attributes of the hinges or the method of actuating the hinges. This section shifts focus towards the hinge design in the physical OSCaR. For the proposed structure in this paper, the hinges must exhibit favorable characteristics in the following aspects.

- Degree of freedom. Having only one degree of freedom is most desirable, since the more degrees of freedom a mechanism has, the more complex its hinge design becomes due to the increased actuation demands.
- Degree of drivability. Achieving motion in mechanisms of this scale is most effectively achieved through servo motors, which output torque on rotatable pivots. Thus, the degree of drivability pertains to the ease with which rotational movement can be translated into panel movement (It is important to note that a linear movement cannot fold panels for 180 degrees due to singularities). In simple terms, mechanisms featuring pivots exhibit a high degree of drivability, while those lacking pivots have a low degree of drivability.
- Degree of protrusion. In the previous section, the hinge shift technique was employed to accommodate the thickness of the panels, assuming that the hinges are ideal one-dimensional lines. However, in reality, the three-dimensional space occupied by the hinges and their actuators cannot be disregarded. If the pivot is placed in the crease line, it will protrude from the edge, causing collisions of panels where two or more crease lines become colinear, such as the mountain creases in the folded state. Hence, the degree of protrusion delineates the extent to which the mechanism protrudes beyond the edge, as illustrated in Fig. 4 (a). A low degree of protrusion is preferable, as it prevents the panels from collisions.

As a result, the preferable characteristics of the hinge design are one degree of freedom, a high degree of drivability,

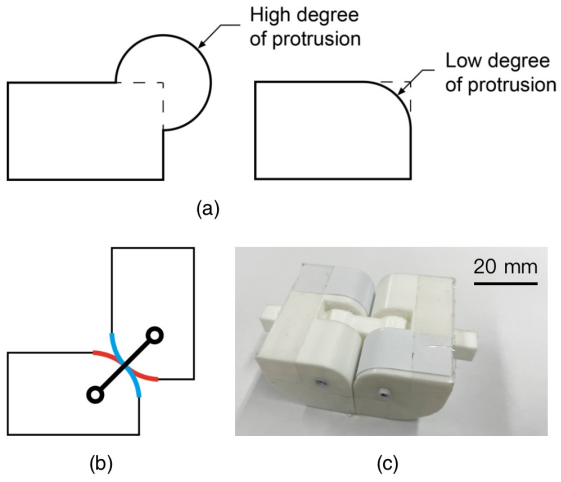

Fig. 4. Explanation of degree of protrusion and the hinge design. (a) Examples of high and low degree of protrusion. (b) Design of rolling contact / doubled hinge combo hinge at an intermediate state. (c) Prototype of rolling contact / doubled hinge combo hinge at the initial state.

and a low degree of protrusion.

Besides the hinge shift techniques, various techniques are available for implementing hinges in thick-panel origami. Common techniques encompass tapered panel [23], offset panel [24], doubled hinge [25], membrane [4], rolling contacts [26], and strained joint [27]. Their profiles are summarized in TABLE II. Hinges constructed using the hinge shift technique, the tapered panel technique or the offset panel technique have one degree of freedom and a high degree of drivability. But their pivots are at the edge of the panels, resulting in a high degree of protrusion. Hinges made with the doubled hinge technique have two degrees of freedom and a high degree of drivability. Since the pivots can be situated within the panels and the link can be made sufficiently thin, they have a low degree of protrusion. Hinges formed using the membrane technique and the strained joint technique have multiple degrees of freedom, as the membrane is flexible. They also exhibit a low degree of drivability and a low degree of protrusion. Hinges made using the rolling contacts technique have one degree of freedom and a low degree of protrusion. But they possess a low degree of drivability. The comparison of these techniques is summarized in TABLE II, with undesirable attributes being highlighted in red.

The evaluation of the thickness-accommodation techniques indicates that none of the hinge designs fulfill the requirements independently. Therefore, a combination of techniques was employed. The combo hinge design has cylindrical rolling contacts on each side of the panel and a link connecting the centerlines of the cylindrical surfaces, as shown in Fig. 4 (b). The rolling contacts can be constructed with a pair of flexible materials shown as the blue and red curves in Fig. 4 (b). Such material can be in either membrane or wire forms. Combining the strength of both techniques, the hinges offer one degree of freedom a low degree of protrusion, and can be actuated by adding a torsional actuator at one of the pivots of the links. A prototype of the combo hinge hinge is presented in Fig. 4 (c).

TABLE II
COMPARISON OF THICKNESS-ACCOMMODATION TECHNIQUES

Technique	Schematic	Degree of freedom	Degree of drivability	Degree of protrusion
Hinge shift		1	high	high
Tapered panel		1	high	high
Offset panel		1	high	high
Doubled hinge		2	high	low
Membrane		n	low	low
Strained joint		n	high	low
Rolling contacts		1	low	low
Rolling contact + doubled hinge		**1**	**high**	**low**

III. SYSTEM DESIGN

A. Structure

The structure design of OSCaR is illustrated in Fig. 5 (a). The prototype employs the folding structure and the rolling contact / doubled hinge combo hinge design presented in the previous chapter.

To accommodate varying crease lengths and simplify the fabrication process, a modular approach was adopted for the prototype's design. Each panel consists of two acrylic plates (light gray) at the top and bottom along with a set of hinges. For each crease, two rolling-contact modules (orange) are placed at the two ends and a dual-pivot hinge module (yellow) is placed in the middle, forming a stable rolling contacts / doubled hinge combo hinge. The servos (red) for actuation are mounted on the 3 slightly modified dual-pivot hinges in the square panel. A majority of the hinge components in the hinges are 3D printed using PLA material.

The robot's locomotion is based on a differential drive system. It comprises two actuated wheels (black) powered by DC motors (purple) and three casters wheels (blue). The 2 actuated wheels are mounted on the square panel, and a caster is mounted in front of them. Additionally, each of the two rectangular panels is equipped with a caster to offer supplementary support when deployed.

Fig. 5 (b) shows the structure design of the rolling-contact module and dual-pivot module. The rolling-contact module uses a pair of PE wires (red) to form the rolling contacts, chosen for its low ductility characteristics. The dual-pivot hinge module incorporates an acrylic link (indigo) and a pair of headed pins (dark gray) serving as pivot points.

B. Hardware

As shown in Fig. 6 (a), the hardware system is built around an ESP32 microcontroller, which is connected to a

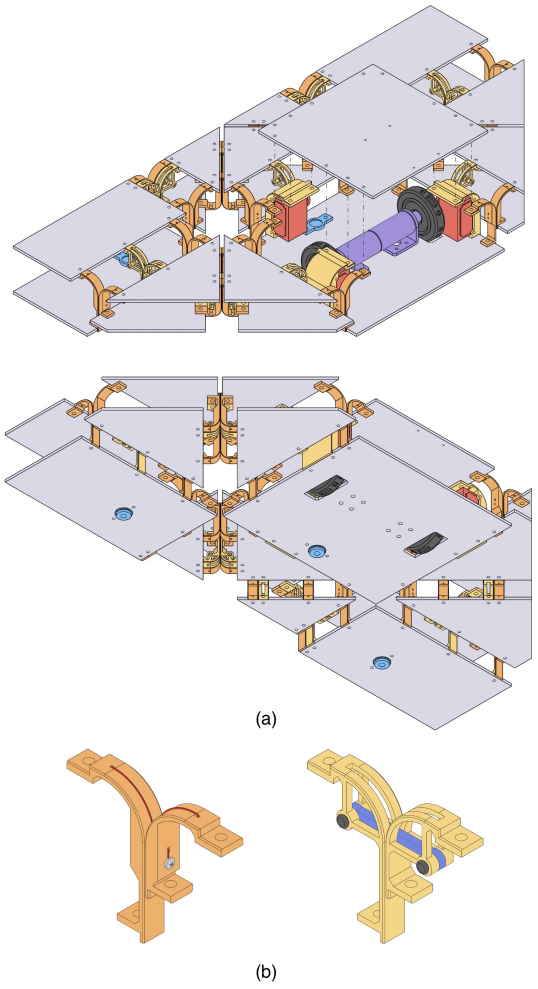

Fig. 5. Structure of OSCaR. (a) Isometric view of the overall structure from the top and bottom sides. (b) Structure of the rolling-contact module and dual-pivot module.

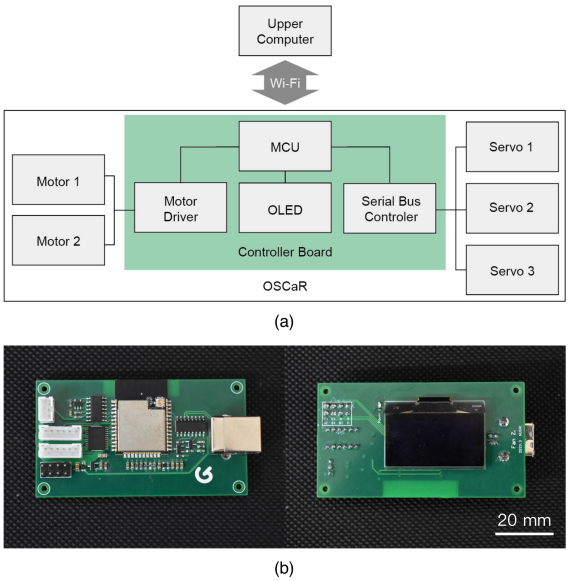

Fig. 6. Hardware system of OSCaR. (a) Hardware system structure. (b) Controller board from the top and bottom view.

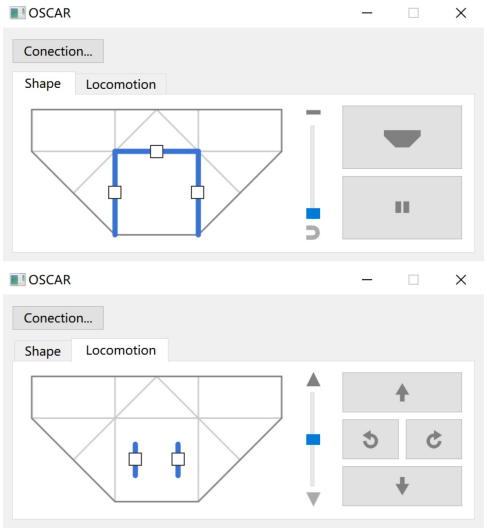

Fig. 7. Graphical user interface of the upper computer software in ”Shape” tab and ”Locomotion” tab.

motor driver, an OLED display, and a serial bus controller. The motor driver interfaces with the 3 motors responsible for the locomotion; the OLED display is for showing the status of the robot; and the serial bus controller interfaces with the 3 servos, which have built-in controllers that ensure the synchronization of the shape-changing motion. The electronic components are integrated into a single controller board shown in Fig. 6 (b), which can be easily mounted to the prototype. Additionally, the controller can communicate with an upper computer via Wi-Fi, affording wireless control capabilities to govern the prototype’s operations.

C. Software

For the purpose of experiments and demonstrations, an application was developed to facilitate control of the prototype through an upper computer. This application is constructed using the Qt6 framework and enables the transmission of commands to the prototype via a Wi-Fi connection. Its user interface is shown in Fig. 7. The interface comprises two tabs, each dedicated to controlling distinct aspects: the shape and the locomotion of the prototype. Within each tab, a graphical representation of the robot is presented on the left side, depicting its controllable components. These components are equipped with checkboxes, allowing users to select them for manipulation. Adjacent to the diagram, a slider is provided, which users can adjust to modulate the corresponding component’s behavior. In addition to these interactive controls, a set of buttons is positioned on the right-hand side of the interface. These buttons offer users the capability to execute predefined functions, such as folding or moving forward. This application streamlines the process of testing and demonstration.

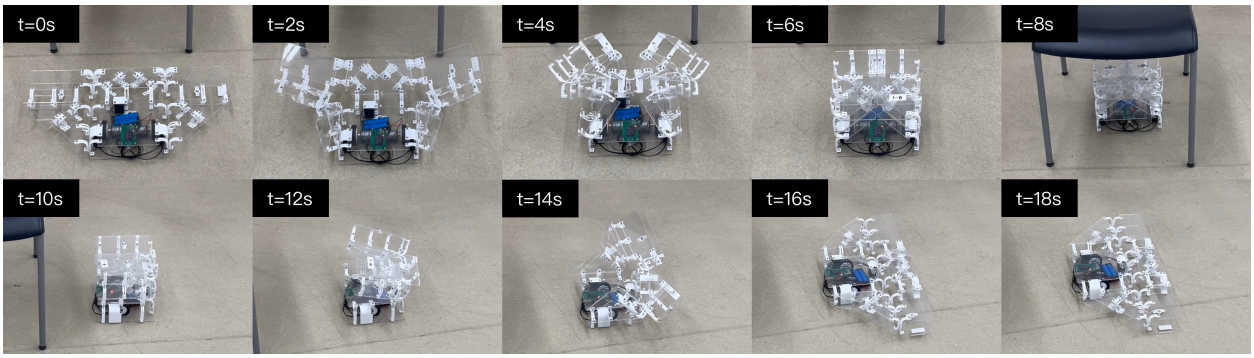

Fig. 8. OSCaR passing through a chair with its shape-changing capabilities.

IV. Experiments and Discussion

The proposed robot is capable of changing its shape into two distinct configurations and moving across the ground in either configuration. Fig. 8 captures the sequential process through which the robot transitions between folded and unfolded states to effectively pass through a chair. In the scenario, the robot employs the deployed configuration in the open area, folding itself and traversing through the tight space between the legs of a chair. Upon clearing the obstacle, it unfolds back to the deployed configuration. This demonstrates the excellent adaptability of OSCaR: expansive coverage efficiency in the deployed position and enhanced maneuverability in the folded configuration.

The design of this structure does pose one limitation: as the robot undergoes folding, the height increases and limits the minimum height the robot can pass through. However, this limitation is not of significant concern, as height constraints are generally less common in comparison to width constraints, especially in outdoor applications. Moreover, this tradeoff is inevitable. Since The robot's overall volume is predominantly dictated by the spatial requirements of its embedded components for certain tasks (e.g. cleaning equipment in a cleaning robot), the height of the robot is inversely proportional to the footprint. So the reduction of footprint will inevitably lead to increased height. For OSCaR, the shape in the folded configuration is designed to be an approximate cube, achieving a balance between its height and footprint.

V. Conclusions and Future Work

This paper proposes an origami-inspired shape-changing robot. The objective is to enhance the adaptability of ground vehicles for coverage tasks in both wide and narrow spaces. The folding pattern has a remarkable deploy-to-stow ratio of 3 in the width direction, and a kinematic model is established for the pattern to simulate the shape-changing process and guide actuation design. The hinges are designed to fold without collision among the panels and be easy to actuate. The system design of the prototype is also presented, encompassing various facets such as the structure, the hardware, and the software. The results show that the robot has great adaptability in complex environments, making it ideal for work that involves covering an area within a set amount of time, such as floor cleaning.

In the context of shape-changing robots like the one proposed, an uncommon characteristic emerges compared to fixed-configuration robots: a substantial proportion of the surfaces undergo orientation changes during folding. This raises a new challenge for attaching sensors to these robots. Moreover, the conventional path planning algorithms, conventionally tailored for robots with a fixed configuration, may encounter compatibility issues when applied to shape-changing robots. Future work will delve into devising localization methods and path-planning strategies for this kind of shape-changing robot.

References

[1] M. Meloni, J. Cai, Q. Zhang, D. Sang-Hoon Lee, M. Li, R. Ma, T. E. Parashkevov, and J. Feng, "Engineering origami: A comprehensive review of recent applications, design methods, and tools," *Advanced Science*, vol. 8, no. 13, p. 2000636, 2021.

[2] L. M. Fonseca, G. V. Rodrigues, and M. A. Savi, "An overview of the mechanical description of origami-inspired systems and structures," *International Journal of Mechanical Sciences*, vol. 223, p. 107316, 2022.

[3] J. Back, B. Schuettpelz, A. Ewing, and G. Laue, "James webb space telescope sunshield membrane assembly," in *50th AIAA/ASME/ASCE/AHS/ASC Structures, Structural Dynamics, and Materials Conference 17th AIAA/ASME/AHS Adaptive Structures Conference 11th AIAA No*, 2009, p. 2156.

[4] S. A. Zirbel, R. J. Lang, M. W. Thomson, D. A. Sigel, P. E. Walkemeyer, B. P. Trease, S. P. Magleby, and L. L. Howell, "Accommodating thickness in origami-based deployable arrays," *Journal of Mechanical Design*, vol. 135, no. 11, p. 111005, 2013.

[5] S. Attia, "Evaluation of adaptive facades: The case study of al bahr towers in the uae," *QScience Connect*, vol. 2017, no. 2, p. 6, 2017.

[6] S. Felton, M. Tolley, E. Demaine, D. Rus, and R. Wood, "A method for building self-folding machines," *Science*, vol. 345, no. 6197, pp. 644–646, 2014.

[7] K. Kuribayashi, K. Tsuchiya, Z. You, D. Tomus, M. Umemoto, T. Ito, and M. Sasaki, "Self-deployable origami stent grafts as a biomedical application of ni-rich tini shape memory alloy foil," *Materials Science and Engineering: A*, vol. 419, no. 1-2, pp. 131–137, 2006.

[8] S. Miyashita, S. Guitron, K. Yoshida, S. Li, D. D. Damian, and D. Rus, "Ingestible, controllable, and degradable origami robot for patching stomach wounds," in *2016 IEEE international conference on robotics and automation (ICRA)*. IEEE, 2016, pp. 909–916.

[9] D.-Y. Lee, J.-S. Kim, S.-R. Kim, J.-S. Koh, and K.-J. Cho, "The deformable wheel robot using magic-ball origami structure," in *International Design Engineering Technical Conferences and Computers and Information in Engineering Conference*, vol. 55942. American Society of Mechanical Engineers, 2013, p. V06BT07A040.

[10] S. Miyashita, S. Guitron, M. Ludersdorfer, C. R. Sung, and D. Rus, "An untethered miniature origami robot that self-folds, walks, swims, and degrades," in *2015 IEEE international conference on robotics and automation (ICRA)*. IEEE, 2015, pp. 1490–1496.

[11] J. T. Karras, C. L. Fuller, K. C. Carpenter, A. Buscicchio, D. McKeeby, C. J. Norman, C. E. Parcheta, I. Davydychev, and R. S. Fearing, "Pop-up mars rover with textile-enhanced rigid-flex pcb body," in *2017 IEEE International Conference on Robotics and Automation (ICRA)*. IEEE, 2017, pp. 5459–5466.

[12] S. Li, J. J. Stampfli, H. J. Xu, E. Malkin, E. V. Diaz, D. Rus, and R. J. Wood, "A vacuum-driven origami "magic-ball" soft gripper," in *2019 International Conference on Robotics and Automation (ICRA)*. IEEE, 2019, pp. 7401–7408.

[13] C. H. Belke, K. Holdcroft, A. Sigrist, and J. Paik, "Morphological flexibility in robotic systems through physical polygon meshing," *Nature Machine Intelligence*, pp. 1–7, 2023.

[14] Z. Wang, Y. Song, Z. Wang, and H. Zhang, "Origami folding enhances modularity and mechanical efficiency of soft actuators," in *2023 IEEE International Conference on Robotics and Automation (ICRA)*. IEEE, 2023, pp. 648–654.

[15] S. Okada, K. Ishizawa, and Y. Murai, "Development of internal investigation device for primary containment vessel. shape changing robot'pmorph'," *Denki Hyoron*, vol. 102, no. special issue, pp. 27–31, 2017.

[16] V. Prabakaran, M. R. Elara, T. Pathmakumar, and S. Nansai, "htetro: A tetris inspired shape shifting floor cleaning robot," in *2017 IEEE International Conference on Robotics and Automation (ICRA)*. IEEE, 2017, pp. 6105–6112.

[17] C. Zheng and K. Lee, "Wheeler: Wheel-leg reconfigurable mechanism with passive gears for mobile robot applications," in *2019 International Conference on Robotics and Automation (ICRA)*. IEEE, 2019, pp. 9292–9298.

[18] R. Suzuki, C. Zheng, Y. Kakehi, T. Yeh, E. Y.-L. Do, M. D. Gross, and D. Leithinger, "Shapebots: Shape-changing swarm robots," in *Proceedings of the 32nd annual ACM symposium on user interface software and technology*, 2019, pp. 493–505.

[19] T. Tachi, "Geometric considerations for the design of rigid origami structures," in *Proceedings of the International Association for Shell and Spatial Structures (IASS) Symposium*, vol. 12, no. 10. Elsevier Ltd Shanghai, China, 2010, pp. 458–460.

[20] H. Feng, R. Peng, J. Ma, and Y. Chen, "Rigid foldability of generalized triangle twist origami pattern and its derived 6r linkages," *Journal of Mechanisms and Robotics*, vol. 10, no. 5, p. 051003, 2018.

[21] G. Wei and J. S. Dai, "Origami-inspired integrated planar-spherical overconstrained mechanisms," *Journal of Mechanical Design*, vol. 136, no. 5, p. 051003, 2014.

[22] Y. Chen, R. Peng, and Z. You, "Origami of thick panels," *Science*, vol. 349, no. 6246, pp. 396–400, 2015.

[23] T. Tachi, "Rigid-foldable thick origami," *Origami*, vol. 5, pp. 253–264, 2011.

[24] B. J. Edmondson, R. J. Lang, S. P. Magleby, and L. L. Howell, "An offset panel technique for thick rigidily foldable origami," in *International Design Engineering Technical Conferences and Computers and Information in Engineering Conference*, vol. 46377. American Society of Mechanical Engineers, 2014, p. V05BT08A054.

[25] J. S. Ku and E. D. Demaine, "Folding flat crease patterns with thick materials," *Journal of Mechanisms and Robotics*, vol. 8, no. 3, p. 031003, 2016.

[26] R. J. Lang, T. Nelson, S. Magleby, and L. Howell, "Thick rigidly foldable origami mechanisms based on synchronized offset rolling contact elements," *Journal of Mechanisms and Robotics*, vol. 9, no. 2, p. 021013, 2017.

[27] N. A. Pehrson, S. P. Magleby, R. J. Lang, and L. L. Howell, "Introduction of monolithic origami with thick-sheet materials," in *Proceedings of IASS Annual Symposia*, vol. 2016, no. 13. International Association for Shell and Spatial Structures (IASS), 2016, pp. 1–10.